Self-Foldable Supramolecular Polymers

Folding is an important organization process for proteins which allows them to perform intricate functions. Replicating this process for supramolecular polymers, however, remains a challenging task, as their backbones are based on non-covalent bonds. Here, we report an unprecedented supramolecular polymer system, wherein initially formed misfolded structures self-fold to yield a topology reminiscent of protein tertiary structures. Thermodynamic analysis revealed that the folding is accompanied by a large enthalpic gain. Mechanistic insights revealed that self-folding proceeds via ordering of misfolded domains in the main chain using helical domains as templates.

Figure 1 shows the molecular structures of supramolecular monomers **1-3**. Our group previously discovered that **1** can form uniform toroidal nanofibers by hydrogen-bond assisted supramolecular hexamerization of barbiturate units followed by stacking of the resulting hexamers (rosettes) with intrinsic curvature [1, 2]. Further expanding the molecular structure to **2**, we succeeded in engineering helically folded supramolecular polymers (SP) that can be converted into misfolded fibers by photo-irradiation [3, 4]. However, the misfolded fibers did not recover the original folded structures by any means other than thermal reconstruction. We infer that the increased conformational flexibility of the molecular structure impaired the degree of internal order in the supramolecular polymer backbone, making it difficult to reorganize into the helically folded structures. Accordingly, a more rigid monomer scaffold could improve the degree of internal order of the supramolecular polymer backbone which led us to molecule **3** after examining several potential candidates. Folding of supramolecular polymers of **3** proceeds on a long time scale, which enabled us to directly visualize intermediate states of the topological transition using atomic force microscopy (AFM) [5].

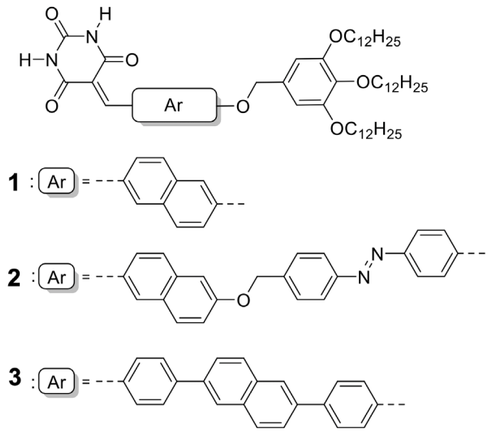

Figure 1: Molecular structures of supramolecular monomers **1-3**.

Slow cooling (1.0 K min^{-1}) of a hot methylcyclohexane (MCH) solution of **3** resulted in the formation of misfolded SP with minor amounts of helically folded conformations [**Fig. 2(A)**]. The resultant solution upon aging at room temperature exhibited a unique self-folding phenomenon of the misfolded domains into helical domains [**Fig. 2(B)**], whereby eventually fully bundled helices with uniform curvature radii (13 ± 1 nm) and persistent length (170–340 nm), reminiscent of the protein's higher-order topologies, were obtained in quantitative yield over a time period of 5–7 days [**Fig. 2(C)**]. Moreover, these fully bundled helices were interlinked by "turn segments" (dotted squares) [inset, **Fig. 2(C)**]. Further morphological transformations were not observed even after prolonged aging, suggesting that these fully bundled helices constitute the global minimum in the energy landscape. Interestingly, upon cooling the same MCH solution of **3** at a much faster cooling rate (e.g., 10 K min^{-1}), fully misfolded shorter SPs with more inhomogeneous curvature radii (14 ± 4 nm) were obtained [**Fig. 2(D)**]. Surprisingly, no morphological evolution over time was observed, suggesting that these fully misfolded SPs are kinetically trapped species. Furthermore, the solutions obtained by mixing separately prepared solutions of fully folded and fully misfolded SPs also did not show any evolution over time, suggesting that the misfolded SPs do not self-fold, neither via an external template mechanism nor by depolymerization–polymerization via monomer exchange. Accordingly, self-folding occurs only when misfolded and folded domains exist in the same SP chain wherein the termini of the helical domains act as a "definite curvature template" for the folding of tethered misfolded chains.

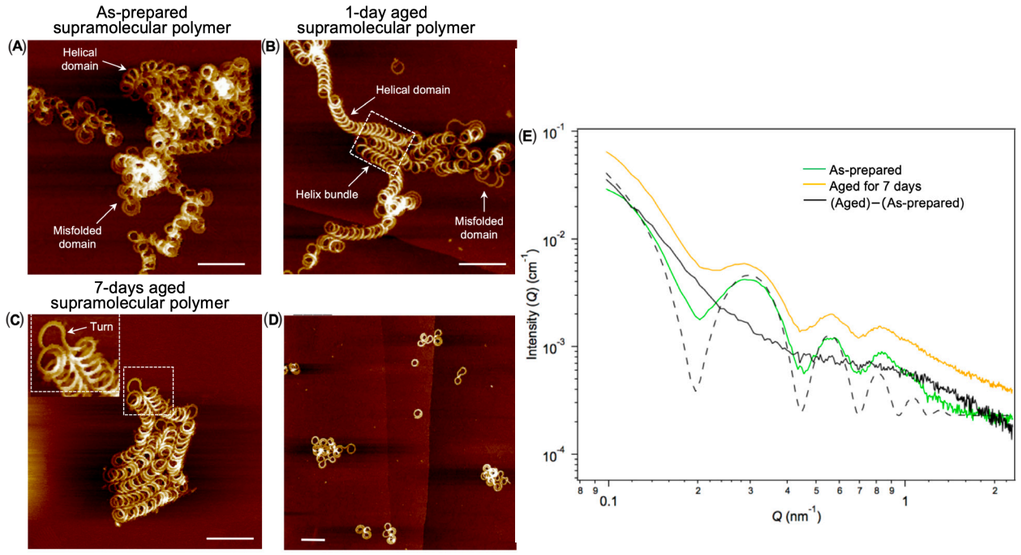

Figure 2: (A to **C)** AFM images showing the self-folding process of the supramolecular polymers of **3**, after aging the solution at 293 K for 0 min **(A)**, 1 day **(B)**, and 7 days **(C)**. Scale bars, 100 nm. The inset in **(C)** shows a magnification of the turn segment enclosed by the dotted square. **(D)** AFM image of fully misfolded supramolecular polymers. Scale bars, 100 nm. **(E)** SAXS profiles of the as-prepared solution (green curve) and the 7-day-old solution (orange curve) of **3** ($c = 5 \times 10^{-5}$ M) prepared at a cooling rate of 1.0 K min^{-1}. The black curve is the profile obtained by subtracting the two data sets. The black dashed curve is a simulation SAXS profile of the as-prepared sample data using a hollow cylinder model.

The self-folding phenomenon of the above SPs was further probed in solution using small-angle X-ray scattering (SAXS). Both as-prepared supramolecular polymer solution and aged sample displayed identical scattering peaks within the range Q = 0.2 to 0.9 nm^{-1}, except the latter showed an increase in SAXS intensity throughout the Q range [**Fig. 2(E)**]. Data analysis using a hollow cylinder model [**Fig. 2(E)**, dashed curve] provided an average curvature radius of 12.3 nm, which is in agreement with the dimensions measured by AFM. Subtracting the fresh SAXS data from that collected for the aged sample (**Fig. 2(E)**, black curve) resulted in a smooth curve with no observable maxima/minima, suggesting that within this probed size range (Q = 0.2 to 0.9 nm^{-1} corresponding to 30 to 7 nm), there is no major change in the structure (that is, it remains, on average, in the coiled state). Also, the subtracted data at $Q < 0.2$ nm^{-1} exhibit a region where $I(Q) \approx Q^{-3}$ and another additional broad contribution centered around Q = 0.9 nm^{-1}. Because of the limitations of modeling such a complex structure, neither of these features can presently be unambiguously assigned, although the power-law scattering is likely to derive from the more open, equilibrated structures observed by AFM after aging.

REFERENCES

[1] S. Yagai, Y. Goto, X. Lin, T. Karatsu, A. Kitamura, D. Kuzuhara, H. Yamada, Y. Kikkawa, A. Saeki and S. Seki, *Angew. Chem. Int. Ed.* **51**, 6643 (2012).
[2] M. J. Hollamby, K. Aratsu, B. R. Pauw, S. E. Rogers, A. J. Smith, M. Yamauchi, X. Lin and S. Yagai, *Angew. Chem. Int. Ed.* **55**, 9890 (2016).
[3] B. Adhikari, Y. Yamada, M. Yamauchi, K. Wakita, X. Lin, K. Aratsu, T. Ohba, T. Karatsu, M. Hollamby, N. Shimizu, H. Takagi, R. Haruki, S. Adachi and S. Yagai, *Nat. Commun.* **8**, 15254 (2017).
[4] B. Adhikari, Y. Yamada, M. Yamauchi, K. Wakita, X. Lin, K. Aratsu, T. Ohba, T. Karatsu, M. Hollamby, N. Shimizu, H. Takagi, R. Haruki, S. Adachi and S. Yagai, *PF Highlights 2017* **31**(2018).
[5] D. D. Prabhu, K. Aratsu, Y. Kitamoto, H. Ouchi, T. Ohba, M. J. Hollamby, N. Shimizu, H. Takagi, R. Haruki, S. Adachi and S. Yagai, *Sci. Adv.* **4**, eaat8466 (2018).

BEAMLINE

BL-15A2

D. D. Prabhu[1], K. Aratsu[1], Y. Kitamoto[1], H. Ouchi[1], T. Ohba[1], M. J. Hollamby[2], N. Shimizu[3], H. Takagi[3], R. Haruki[3], S. Adachi[3] and S. Yagai[1] ([1]Chiba Univ., [2]Keele Univ., [3]KEK-IMSS-PF)